Letters

Asymmetrical-Bidirectional Input-Series–Output-Parallel Modular DC–DC Converter in DC Distribution Grids With Renewables

Changjiang Sun, *Member, IEEE*, Shuai Wang, *Member, IEEE*, Josep Pou, *Fellow, IEEE*, Chandana Jayampathi Gajanayake, *Senior Member, IEEE*, and Amit Kumar Gupta, *Fellow, IEEE*

***Abstract*—Interlinking dc–dc converters are essential in urban-area dc distribution grids to interconnect the medium-voltage and low-voltage (LV) buses. The increasing installation of renewable energy sources at the LV side will result in backward power flow through these converters, which is usually less than the forward power. This letter presents an asymmetrical-bidirectional input-series–output-parallel (AB-ISOP) dc–dc converter with a partial-scale backward power rating to satisfy the above realistic requirement. Single-active bridge (SAB) and dual-active bridge (DAB) converter modules are combined in the proposed structure: the unidirectional SABs process most of the forward power, whereas the bidirectional DABs provide passage for the backward power flow. A string of embedded nonisolated resonant DAB converters is constructed at the input stage to realize natural power coupling and voltage sharing. Compared with the all-DAB ISOP scheme, the proposed one requires fewer devices and presents higher conversion efficiency as active switches are omitted at the secondary side of SABs. Experiments conducted on the down-scale prototype verify the operating principles and performance of the proposed converter.**

***Index Terms*—DC distribution grids, dc-dc converter, dual active bridge (DAB) converter, input-series–output-parallel (ISOP) converter, renewable energy, single active bridge (SAB) converter.**

I. Introduction

With the rapidly increasing penetration of power electronic technologies, most of the loads in the future urban areas will be natural dc or operated with dc internal links [1], such as electric vehicle charging stations, data centers, and inverter interfaced heat pumps or air conditioners. Furthermore, the output of distributed sustainable energy sources such as photovoltaic (PV) and energy storage systems are also in dc mode. Constructing dc distribution grids in urban areas to supply future dc homes and buildings will save conversion stages, reducing losses, and lowering investment costs [2].

A dc distribution grid usually has multiple buses with different voltage levels, i.e., the medium-voltage (MV) and low-voltage (LV) dc buses, among which the LV bus can supply home and building applications and integrate rooftop PV panels [3]. The interlinking dc–dc converter is essential in the urban-area dc grid to interconnect the MV and LV buses and implement voltage or power control [4].

Generally, the power flow direction in the interlinking dc–dc converter is from the MV to the LV bus, and a unidirectional dc–dc converter is sufficient to meet the requirements. However, with the consistently increasing installation capacity of distributed generator systems, such as PV panels, the produced power may exceed the consumption at the LV side during the daytime. Delivering the surplus power to the MV side can reduce the capacity requirement of the energy storage system and enhance the optimal operation of the whole power system. This requires the interlinking dc–dc converter to process the backward power flow, usually less than the forward one [5]. For this scenario, deploying conventional bidirectional converters designed with full-scale power ratings for both directions will result in low switch utilization and unnecessary costs. By contrast, an asymmetrical-bidirectional dc–dc converter with a partial-scale backward power rating to link the buses can satisfy the realistic demand with high economic efficiency.

The concept of asymmetrical-bidirectional dc–dc conversion can date back to Meyer's [6] work on the design of a multiphase series-resonant converter for the offshore wind power collection system. Zhu et al. [7] proposed a modified dual-active bridge (DAB) converter with a partially rated active bridge and a diode rectifier paralleled at the secondary side to realize asymmetrical-bidirectional conversion in solid-state transformers. The total cost is reduced with a slight increase in power losses.

The input-series–out-parallel (ISOP) modular dc–dc converter is preferable for linking the MV and LV dc busses owing to its high-voltage and high-current handling capabilities at the input and output sides, respectively [8]. Exhibiting soft-switching

Manuscript received 13 June 2023; revised 17 September 2023; accepted 8 October 2023. Date of publication 3 November 2023; date of current version 16 February 2024. This work was supported by the RIE2022 Industry Alignment Fund-Industry Collaboration Projects Funding Initiative, as well as cash and in-kind contribution from Rolls-Royce Singapore Pte Ltd. *(Corresponding author: Changjiang Sun.)*

Changjiang Sun is with Rolls-Royce@NTU Corporate Lab, Nanyang Technological University, Singapore 639798 (e-mail: changjiang.sun@ntu.edu.sg).

Shuai Wang, Chandana Jayampathi Gajanayake, and Amit Kumar Gupta are with Rolls-Royce Electrical, Rolls-Royce Singapore Pte. Ltd., Singapore 638673 (e-mail: shuai.wang@rolls-royce-electrical.com; chandana.gajanayake@rolls-royce.com; a.gupta@ntu.edu.sg).

Josep Pou is with the School of Electrical and Electronic Engineering, Nanyang Technological University, Singapore 639798 (e-mail: josep.pou@ieee.org).

Color versions of one or more figures in this article are available at https://doi.org/10.1109/TPEL.2023.3329775.

Digital Object Identifier 10.1109/TPEL.2023.3329775

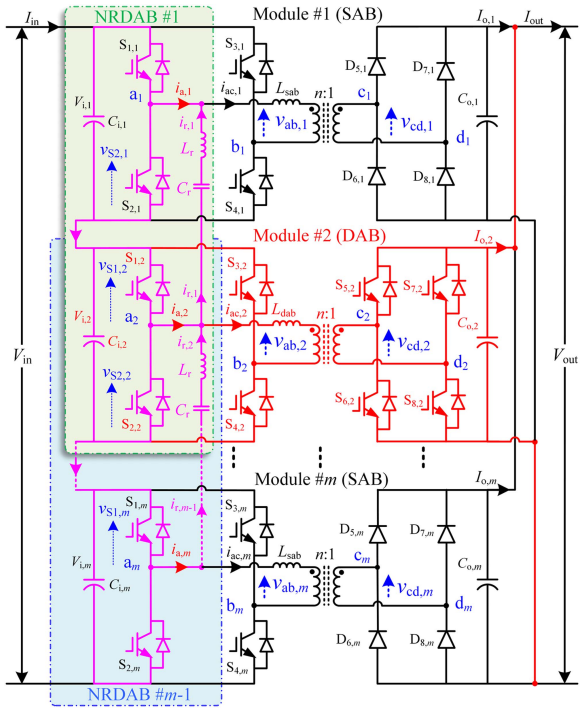

Fig. 1. Configuration of the proposed AB-ISOP system.

properties and providing galvanic isolation with high-frequency transformers, DAB and single-active bridge (SAB) converters, along with their variants [9], [10], [11], are promising constituent modules in an ISOP system. Compared with the DAB converter with active full bridges utilized at both the primary and secondary sides to process bidirectional power, the SAB converter saves the secondary-side active switches, reducing hardware costs significantly but only allowing forward power flow [7].

This letter presents an asymmetrical-bidirectional input-series–output-parallel (AB-ISOP) dc–dc converter composed of SAB and DAB modules. At the input stage, to implement automatic voltage sharing and power equalization technology from [12] and [13], which could be considered as an embedded variant of the independent resonant switched-capacitor ladder used in [14], [15], and [16], a string of nonisolated resonant dual active bridge (NRDAB) converters is constructed by adding *LC* branches to tie every two adjacent modules. The internal power transfer mechanism and system-level configuration principle of SAB and DAB modules in the hybrid structure are illustrated, and a coordinating control strategy is proposed to realize seamless power reversal. Compared with the all-DAB ISOP system with full-scale backward power rating, the proposed one saves hardware cost, simplifies control system, and improves conversion efficiency as active switches are omitted at the secondary side of SAB modules.

II. Topology and Power Transfer Mechanism

A. Topology Description

As shown in Fig. 1, the proposed AB-ISOP converter comprises multiple SAB and DAB modules connected in series at the input side and in parallel at the output side. A DAB module is constructed by a high-frequency transformer and two active full bridges located at both primary and secondary sides, whereas the SAB modules use diode bridges at the secondary side. DABs should be symmetrically dispersed among the SAB modules. The reason will be detailed in the following section. Module #2 is drawn as a DAB in Fig. 1 only for easy illustration.

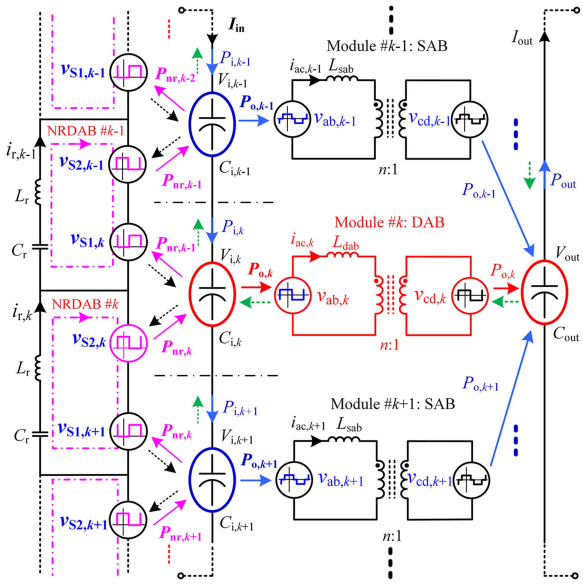

Fig. 2. Equivalent model of the proposed AB-ISOP system.

At the input stage, *LC* branches consisting of L_r and C_r are installed to link the midpoints of two adjacent leading legs. Designed to resonate at the switching frequency, every *LC* network and the connected half bridges from two adjacent modules form an embedded NRDAB converter. All the primary-side leading legs, except the top and bottom ones, are jointly utilized by two adjacent NRDAB converters. This configuration builds up an embedded power coupling and voltage-sharing link chain at the input stage, similar to the embedded output-side voltage-sharing structure in [12] and [13].

B. Circuit Modeling and Power Transfer Mechanism

By assuming the *k*th module is a DAB and its adjacent modules are SABs, the internal power transfer mechanism of the AB-ISOP system is illustrated in Fig. 2, where the input- and output-side capacitors are modeled as energy tanks. According to Fig. 1, when the upper- and lower-arm devices in the primary-side leading leg of each module (e.g., $S_{1,k}$ and $S_{2,k}$ in module #*k*) are switched ON and OFF alternately, square-wave voltage sources (i.e., $v_{S1,k}$ and $v_{S2,k}$) will be produced across the arms. The equivalent voltage sources across adjacent arms from two modules (e.g., $v_{S2,k\text{-}1}$ from module #*k*-1 and $v_{S1,k}$ from module #*k*) interact with each other through the added *LC* tank, forming a resonant power transfer loop. As shown in Fig. 2, the formed NRDAB #*k*-1 enables power exchange ($P_{nr,k\text{-}1}$) between energy tanks $C_{i,k\text{-}1}$ and $C_{i,k}$, and the neighboring NRDAB #*k* facilitates power transfer ($P_{nr,k}$) between energy tanks $C_{i,k}$ and $C_{i,k+1}$. With every two adjacent modules connected by an NRDAB

circuit, a power-sharing link chain is established at the input stage.

In Fig. 2, the transmission power in the kth module is denoted as $P_{\mathrm{o},k}$. Enabled by NRDAB #k, $P_{\mathrm{nr},k}$ represents the power transmission between module #k+1 and module #k. According to the power conservation law, by neglecting conversion losses, the power exchange between the kth module and the input source, i.e., $P_{\mathrm{i},k}$, is expressed as

$$P_{\mathrm{i},k} = P_{\mathrm{o},k} + P_{\mathrm{nr},k-1} - P_{\mathrm{nr},k}. \tag{1}$$

As the input capacitors of all the modules are connected in series to share the input current, to ensure the voltage balance, the capacitors should absorb/release the same amount of power from/to the input-side dc link, which is equal to the average power transmission of all the module, i.e.,

$$P_{\mathrm{i},1}=P_{\mathrm{i},2}=\cdots P_{\mathrm{i},k}=\cdots=P_{\mathrm{i},m}=P_{\mathrm{o,ave}}=\frac{1}{m}\sum_{j=1}^{m}P_{\mathrm{o},j} \tag{2}$$

where m is the number of modules in the ISOP and $P_{\mathrm{o},j}$ represents the delivered power in the jth module.

To ensure the absorb/release power of the energy tank $C_{\mathrm{i},k}$ (i.e., $P_{\mathrm{i,k}}$) is equal to the average power $P_{\mathrm{o,ave}}$, NRDAB #k and #k+1 should cooperate to compensate for the power deviation of module #k (i.e., $\Delta P_{\mathrm{o,k}}$). Therefore

$$P_{\mathrm{nr},k} - P_{\mathrm{nr},k-1} = P_{\mathrm{o},k} - P_{\mathrm{o,ave}} = \Delta P_{\mathrm{o},k}. \tag{3}$$

By extending the derivation process of (3), a series of equations expressing the requirement to compensate for the power deviation in all the modules can be obtained, i.e.,

$$\begin{cases} P_{\mathrm{nr},1} = P_{\mathrm{o},1} - P_{\mathrm{o,ave}} = \Delta P_{\mathrm{o},1} \\ P_{\mathrm{nr},2} - P_{\mathrm{nr},1} = P_{\mathrm{o},2} - P_{\mathrm{o,ave}} = \Delta P_{\mathrm{o},2} \\ \cdots \\ P_{\mathrm{nr},k-1} - P_{\mathrm{nr},k-2} = P_{\mathrm{o},k-1} - P_{\mathrm{o,ave}} = \Delta P_{\mathrm{o},k-1} \\ P_{\mathrm{nr},k} - P_{\mathrm{nr},k-1} = P_{\mathrm{o},k} - P_{\mathrm{o,ave}} = \Delta P_{\mathrm{o},k}. \end{cases} \tag{4}$$

Calculating the sum of the equations in (4) by adding their left-hand and right-hand sides, respectively, leads to

$$P_{\mathrm{nr},k} = \sum_{j=1}^{k} P_{\mathrm{o},j} - kP_{\mathrm{o,ave}} = \sum_{j=1}^{k} \Delta P_{\mathrm{o},j}. \tag{5}$$

Equation (5) indicates that to ensure voltage sharing, the generic NRDAB converter, e.g., NRDAB #k, needs to compensate for the sum of power deviation from module #1 to module #k, which is the total power mismatch of modules at its top side.

Under the forward operation mode, power flows from the MV to the LV side, with all the modules transferring power simultaneously. If the power rating of each module is designed identically as P_{N}, the forward power rating of the whole ISOP system is mP_{N}. $P_{\mathrm{o},k}$ is theoretically equal to $P_{\mathrm{o,ave}}$ when all the modules are controlled to deliver the same amount of power, and the power-sharing link chain only needs to handle the power difference caused by the mismatch of parameters.

Under the backward operation mode, power flows from the LV to the MV side, only through the DAB modules. If the installed number of DAB is m_{dab}, the backward power rating of the whole system will be $m_{\mathrm{dab}}P_{\mathrm{N}}$. The average power $P_{\mathrm{o,ave}}$ $= m_{\mathrm{dab}}P_{\mathrm{o,dab}}/m$, when assuming each DAB module delivers the same power of $P_{\mathrm{o,dab}}$. The power deviation of a DAB module can be calculated as

$$\Delta P_{\mathrm{o,dab}} = P_{\mathrm{o,dab}} - m_{\mathrm{dab}}P_{\mathrm{o,dab}}/m = P_{\mathrm{o,dab}}\left(1 - m_{\mathrm{dab}}/m\right). \tag{6}$$

The power of each SAB module is zero under backward operation mode, and its power deviation can be derived as

$$\Delta P_{\mathrm{o,sab}} = 0 - P_{\mathrm{o,dab}}m_{\mathrm{dab}}/m = -P_{\mathrm{o,dab}}m_{\mathrm{dab}}/m. \tag{7}$$

Equations (6) and (7) reveal that the power deviation of DAB and SAB modules in the backward operation mode are opposite in direction. According to (5), the required power transmission in an NRDAB converter is the sum of power deviation. Instead of grouping the DAB modules, dispersing them among the SAB modules symmetrically can avoid the accumulation of mismatch power to reduce power rating of the resonant circuits.

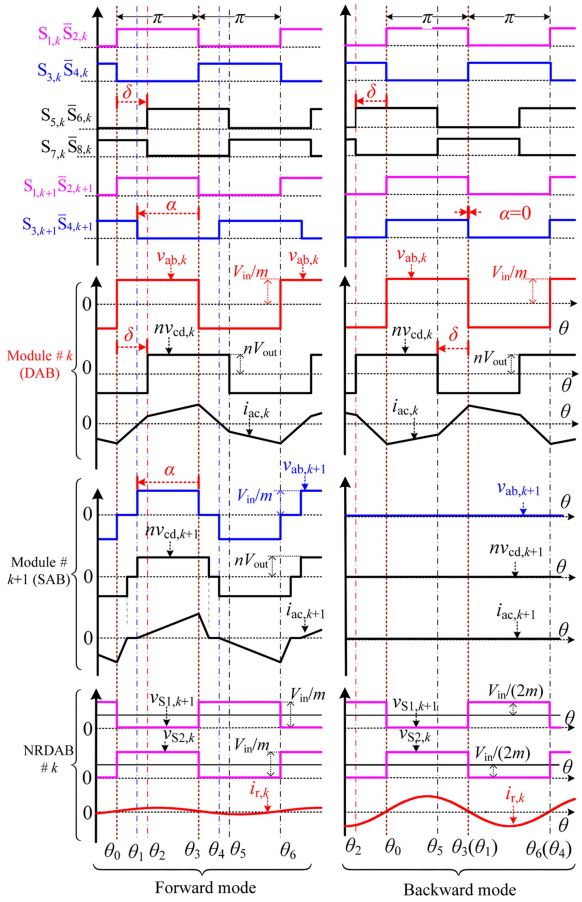

Fig. 3. Operating waveforms of the proposed AB-ISOP converter.

III. Operating Principles and Control Design

A. Bidirectional Power Control in the DAB Module

Fig. 3 illustrates the operating waveforms of the AB-ISOP system by assuming the kth module is a DAB, and its adjacent modules are SABs. Under the classic single-phase shift modulation of DAB, the lagging angle of the secondary voltage (i.e., δ for $nv_{\mathrm{cd},k}$ in module #k) is manipulated to adjust the delivered

power. The active power delivered through a DAB module can be expressed as [9]

$$P_{\mathrm{o,dab}} = nV_{\mathrm{out}}\left(V_{\mathrm{in}}/m\right)\delta\left(\pi - |\delta|\right)/(\pi\omega_{\mathrm{s}}L_{\mathrm{dab}}) \tag{8}$$

in which V_{in}/m is the input voltage of a single module when assuming the voltages are well balanced, V_{out} is the output voltage, L_{dab} represents the lumped ac-side inductance, and ω_{s} is the switching frequency. The transmission power is an odd function of δ, i.e., changing the phase shift direction reverses power flow.

B. Unidirectional Power Transmission in the SAB Module

The phase angle of the lagging-leg voltage at the primary side of SAB is manipulated to control the transferred power. As shown in Fig. 3, switching signals for $S_{3,k+1}$ and $S_{4,k+1}$ in a generic SAB are shifted forward by α relative to driving pulses of the leading leg (i.e., $S_{1,k+1}$ and $S_{2,k+1}$). Under the discontinuous current mode, the delivered power in an SAB module can be expressed as [7]

$$P_{\mathrm{o,sab}} = nV_{\mathrm{out}}\left(V_{\mathrm{in}}/m\right)\alpha^2\left(V_{\mathrm{in}}/(nmV_{\mathrm{out}}) - 1\right)/\left(2\pi\omega_{\mathrm{s}}L_{\mathrm{sab}}\right). \tag{9}$$

The delivered power of an SAB increases along with the inter-leg phase shift angle α and stays zero when $\alpha = 0$. Under the backward operating mode, the phase shift angle for all the SAB modules can be set as 0 to block power transfer.

C. Natural Voltage Sharing Function of the NRDAB Chain

The *LC* circuits tie the primary-side leading leg of every two adjacent modules to form an embedded NRDAB string. As shown in Fig. 3, when these legs are modulated to generate synchronous voltages, the 50%-duty-cycle open-loop control scheme [17] is implemented for the NRDAB. As the impedance of the *LC* resonant tank is near 0 at the switching frequency, any mismatch between the dc-side capacitor voltages will initiate the required resonant current to eliminate it. This natural feedback mechanism manipulates every NRDAB as an ideal transformer with a fixed conversion ratio of 1:1 to equalize the input voltages.

The conversion ratio of the NRDAB #*k*, namely the ratio between input voltages of modules #*k* and #*k*+1, can be expressed as [12]

$$M_{\mathrm{r}} = V_{\mathrm{i},k}/V_{\mathrm{i},k+1} = 1\Big/\sqrt{1 + Q^2\left(\omega_{\mathrm{r}}/\omega_{\mathrm{s}} - \omega_{\mathrm{s}}/\omega_{\mathrm{r}}\right)^2} \tag{10}$$

where ω_{r} is the resonant frequency of the NRDAB, and Q is the quality factor associated with transferred power, expressed as

$$\omega_{\mathrm{r}} = 1\Big/\sqrt{L_{\mathrm{r}}C_{\mathrm{r}}},\ Q = \pi^2 P_{\mathrm{nr},k}\sqrt{L_{\mathrm{r}}/C_{\mathrm{r}}}\Big/\left(2V_{\mathrm{i},k}^2\right). \tag{11}$$

According to (10), M_{r} is always equal to 1 only when $\omega_{\mathrm{r}} = \omega_{\mathrm{s}}$. The impact of deviation in actual resonant frequency caused by parameter mismatch can be eliminated by setting a limit Q_{limit} for Q during parameter design. For instance, if Q is designed to be smaller than 0.3, M_{r} can be kept higher than 0.998 even if the resonant frequency varies by $\pm 10\%$ [12]. According to (11), the limitation on Q can be realized by applying a constraint upon the resonant network parameter design, i.e.,

$$L_{\mathrm{r}}/C_{\mathrm{r}} \le \left(2V_{\mathrm{i},k}^2 Q_{\mathrm{limit}}/\pi^2 P_{\mathrm{nr,max}}\right)^2 \tag{12}$$

where $V_{\mathrm{i,k}}$ is the input module voltage and $P_{\mathrm{nr,max}}$ is the maximum power requirement on NRDAB, which can be calculated by (5).

The above discussion shows that, under the 50%-duty-cycle open-loop control, each NRDAB converter exhibits a robust capability to equalize the input voltages of two adjacent modules. As every two adjacent NRDABs share a half-bridge, a voltage balancing link chain will be built at the stage when all the primary-side leading legs are driven by synchronous pulses, compensating for power mismatch among the modules without any control.

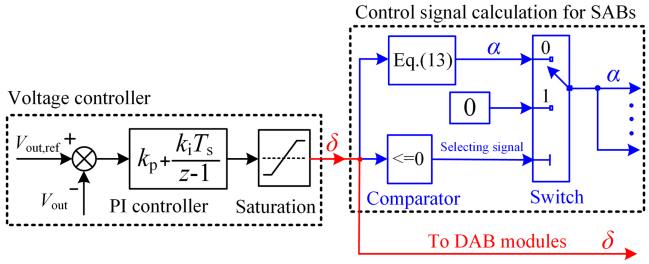

Fig. 4. Control block diagram of the proposed AB-ISOP converter.

D. Coordinating Control for Seamless Power Reversal

One primary system-level requirement for the AB-ISOP converter is establishing and maintaining the LV side voltage. Coordination among different modules is also needed for stable operation. Under the forward mode, to ensure the SAB module transfers the same amount of power as a DAB module, the relationship between α and δ can be derived by combining (8) and (9), i.e.,

$$\alpha = \sqrt{2L_{\mathrm{sab}}\delta\left(\pi - \delta\right)nmV_{\mathrm{out}}/\left(L_{\mathrm{dab}}\left(V_{\mathrm{in}} - nmV_{\mathrm{out}}\right)\right)},\ \text{for}\ \delta > 0. \tag{13}$$

A closed-loop control strategy with coordination among the DAB and SAB modules, as shown in Fig. 4, is implemented for the proposed AB-ISOP converter. A proportional-integral (PI) controller is utilized to maintain the output voltage by adjusting the phase-shift angle of the DAB, i.e., δ. Under the forward mode with $\delta > 0$, the phase shift for SABs is obtained through (13) to follow the transmission power in the DAB. Under the backward mode with $\delta \le 0$, α is kept as 0 to disable power transfer in SABs. With the NRDAB string handling power mismatch among the modules automatically, voltage balancing control is not required under both operating modes. Seamless power reversal without interruption is also achieved when the PI controller manipulates δ to negative values to accommodate the reversed current.

IV. Performance Analysis

A. Current Stress Evaluation

To facilitate analysis, we define the current and power bases in the following equation to normalize the current stresses and

transferred power in the SAB and DAB modules:

$$I_{\text{base}} = (V_{\text{in}}/m)/(2\omega_{\text{s}}L_{\text{dab}});\quad P_{\text{base}} = (V_{\text{in}}/m)^2\Big/(\pi\omega_{\text{s}}L_{\text{dab}}). \tag{14}$$

The ratio between the output voltage (nV_{out}) and the input voltage (V_{in}/m) of a single module is defined as k, and the ratio of SAB ac-side inductance (L_{sab}) to DAB ac-side inductance (L_{dab}) is defined as λ, i.e.,

$$k = nV_{\text{out}}/(V_{\text{in}}/m);\quad \lambda = L_{\text{sab}}/L_{\text{dab}}. \tag{15}$$

Under forward mode, based on (8) and (9), the transmission power of the SAB and DAB modules can be normalized and simplified as

$$\begin{cases} p_{\text{o,dab}} = P_{\text{o,dab}}/P_{\text{base}} = k\delta\left(\pi - |\delta|\right) \\ p_{\text{o,sab}} = P_{\text{o,sab}}/P_{\text{base}} = \alpha^2\left(1-k\right)/(2\lambda) \end{cases}. \tag{16}$$

According to the piecewise expression of inductor current in SAB and DAB converters [7], [9], for $k<1$ the normalized module current stresses referred to the primary side are derived as

$$\begin{cases} i_{\text{peak,dab}} = I_{\text{peak,dab}}/I_{\text{base}} = k(2\left|\delta\right| - \pi) + \pi \\ i_{\text{peak,sab}} = I_{\text{peak,sab}}/I_{\text{base}} = 2\left(1-k\right)\alpha/\lambda \end{cases}. \tag{17}$$

By expressing α and δ as functions of $p_{\text{o,dab}}$ and $p_{\text{o,sab}}$ in (16) and substituting the results into (17), we can obtain the relationship between current stresses and transmission power in each module

$$\begin{cases} i_{\text{peak,dab}} = \pi - k\sqrt{\pi^2 - 4|p_{\text{o,dab}}|/k}, & \text{under } |p_{\text{o,dab}}| \le k\pi^2/4 \\ i_{\text{peak,sab}} = 2\sqrt{2\left(1-k\right)p_{\text{o,sab}}/\lambda}, & \text{under } p_{\text{o,sab}} < \pi^2\left(1-k\right)/(2\lambda) \end{cases}. \tag{18}$$

Under backward mode, the current in the primary-side leading leg of DAB is the superposition of the transformer current and the resonant current. As the resonant circuit connecting with DAB releases power to the neighboring modules, the resonant current is in the opposite direction with the transformer current, reducing the current stress in the primary-side leading leg. Therefore, the maximum current appears in the lagging leg and equals the peak transformer current, which can be obtained by substituting a negative $p_{\text{o,dab}}$ in (18). The transformer current in SAB under the backward mode is zero. The amplitude of resonant current flowing through the primary-side leading legs of SABs, which can be calculated from the equivalent circuit of NRDAB [12], is determined by the maximum transmission power in NRDAB

$$I_{\text{peak,nr}} = \pi P_{\text{nr,max}}/(V_{\text{in}}/m). \tag{19}$$

According to (5), the transmission power in an NRDAB, which is the sum of power deviation in modules on top of itself, is affected by the distribution pattern of DAB and SAB modules. Considering a three-module AB-ISOP with 1 DAB, when the DAB module is placed at the top and middle sides, $P_{\text{nr,max}}$ can be calculated as $P_{\text{o,dab}}/3$ and $2P_{\text{o,dab}}/3$, respectively. Under these scenarios, the normalized current stress in NRDAB is derived as

$$i_{\text{peak,nr}} = \frac{I_{\text{peak,nr}}}{I_{\text{base}}} = \begin{cases} 4p_{\text{o,dab}}/3, \text{when DAB is placed at top} \\ 2p_{\text{o,dab}}/3, \text{when DABis placed at middle} \end{cases}. \tag{20}$$

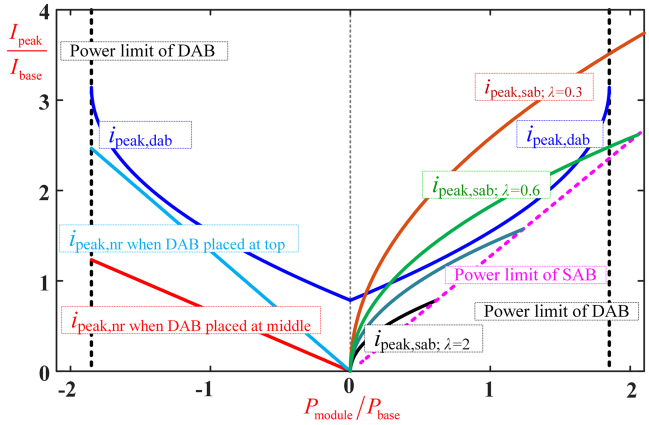

Fig. 5. Curves of primary-side current stresses versus transmission power of single module under different design scenarios.

Based on (18) and (20), Fig. 5 plots the curves of normalized peak currents versus the transmission power of each module, with the voltage ratio k specified as 0.75. In the forward mode, the primary-side current stress in an SAB is usually lower than that of a DAB under light load conditions. Designing a larger ac-side inductor to increase λ can reduce the current stress in an SAB but lower the power transfer capability. Under the backward power flow condition, for three-module AB-ISOP with one DAB, the resonant current amplitude is always lower than that in the DAB. Placing the DAB in the middle reduces the current stress, agreeing with the power transfer mechanism analysis.

B. Soft-Switching Features

The soft-switching condition of a half-bridge unit is mainly determined by the direction of the current at its ac terminal during the switch transition processes. Devices in the AB-ISOP structure, except for the primary-side leading leg, are switched under identical conditions as that in individual DAB or SAB modules. For a primary-side leading leg, the midpoint current is the superposition of the transformer current and resonant current of NRDAB. Similar to that in [12], the resonant current in each NRDAB is nearly zero during switching transitions, having almost no contribution to the commutation current. Therefore, the AB-ISOP system inherits the soft-switching features of individual DAB and SAB converters.

V. Experimental Results

A downscale prototype of the AB-ISOP converter composed of three modules has been fabricated and tested. The first and third modules, from top to bottom, are SABs, while the second is a DAB. Each module's input and output voltages are 70 V and 60 V, respectively, constructing a 210-V to 60-V ISOP converter. With the nominal power of the SAB and DAB designed as 200 W and ±200 W, respectively, the power range of the whole system is from −200 to 600 W. The main circuit parameters of the test converter are listed in Table I, and a photograph of the prototype is shown in Fig. 6.

TABLE I
POWER-CIRCUIT PARAMETERS OF THE AB-ISOP PROTOTYPE

Parameters	Values
Input voltage: V_{in}	210 V
Output voltage: V_{out}	60 V
Number of DAB modules: m_{dab}	1
Number of SAB modules: m_{sab}	2
Turns ratio of transformers: n	1:1
Ac-link inductor of DAB: L_{dab}	150 μH
Ac-link inductor of SAB: L_{sab}	19 μH
Switching frequency: f_s	10 kHz
Resonant capacitor: C_r	20 μF
Resonant inductor: L_r	13 μH

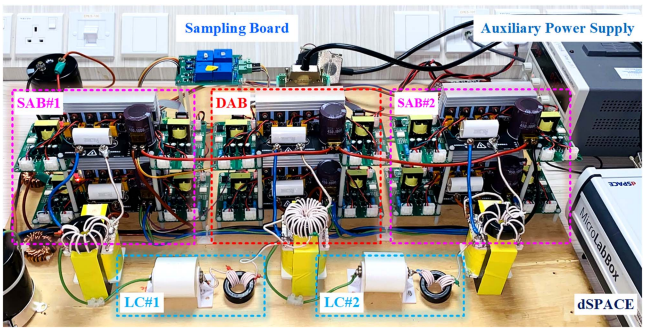

Fig. 6. Photograph of tested AB-ISOP converter prototype.

In the experiment, the tested AB-ISOP controls the output voltage. A programmable power supply maintains the input-side voltage with a resistor paralleled to provide the path for reversed current. Another dc power supply and an electronic load, both operated under current control mode, are deployed at the output side to inject and absorb current, respectively. When the absorbed current drops lower than the injected one, power reversal occurs in the AB-ISOP converter.

Fig. 7(a) and (b) shows the steady-state waveforms when the AB-ISOP transfers the power of +600 W and −200 W, respectively, including the ac-side voltages and currents of an SAB (module #1) and a DAB (module #2) and the resonant currents and ac-terminal voltages of the NRDABs. In forward mode, the SAB and DAB modules deliver power simultaneously with small resonant current ($i_{r,1}$ and $i_{r,2}$) flows in NRDABs. In backward mode, the phase shift angle in the DAB is reversed, whereas the primary and secondary voltages of the SAB are minimized with α set as 0, clamping the transformer current at zero. Sinusoidal resonant currents in NRDABs are increased automatically to handle power mismatches among different modules.

Fig. 8 illustrates the soft-switching feature of devices in the AB-ISOP by capturing the gating signals ($v_{g,S1}$ and $v_{g,S2}$), device voltages (v_{S1} and v_{S2}), and ac-terminal current (i_a) of the primary-side leading leg in DAB and SAB modules. Under the forward power flow condition of 600 W, as shown in Fig. 8(a), the measured waveforms resemble that of individual SAB and DAB converters, as the resonant current is around zero. The voltages across devices are clamped to zero before they are gated on. ZVS turn-ON is thus realized for both SAB and DAB modules. Under the backward power flow condition of −200 W,

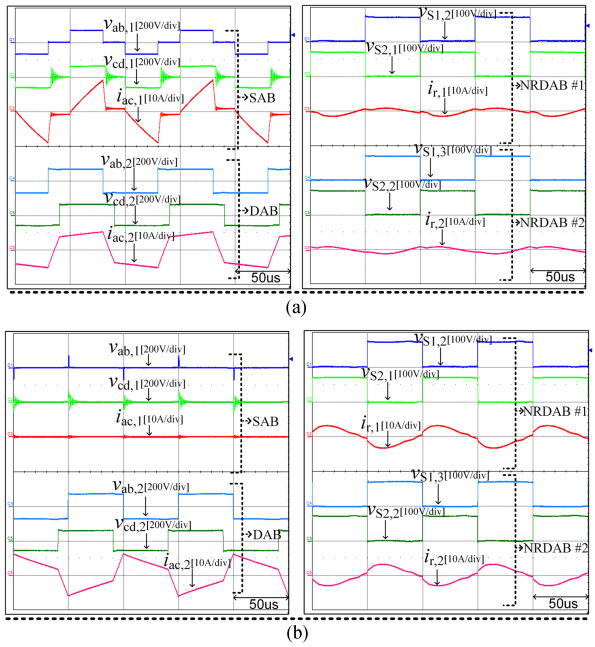

Fig. 7. Measured steady-state waveforms of the AB-ISOP. (a) Forward operating mode. (b) Backward operating mode.

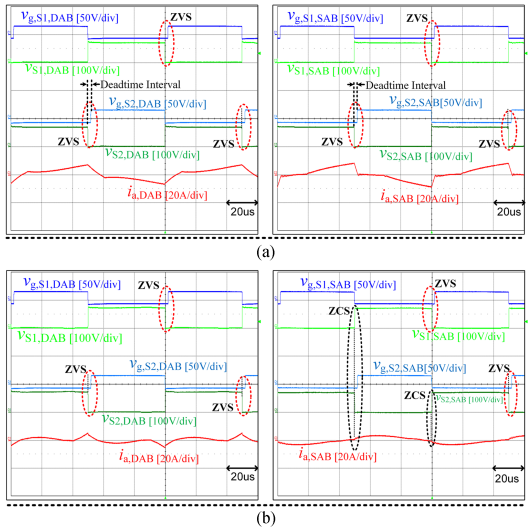

Fig. 8. Measured gating signals ($v_{g,S1}$ and $v_{g,S2}$), device voltages (v_{S1} and v_{S2}), and ac-terminal current (i_a) of the primary-side leading leg in DAB and SAB modules. (a) Forward operating mode. (b) Backward operating mode.

as shown in Fig. 8(b), the ac-terminal current of the leading leg in SAB and DAB modules are the resonant current and the superposition of transformer current and resonant current, respectively. ZCS turn-OFF is achieved in the leading leg of SAB, as the resonant current is around 0 when the devices are gated off. ZVS turn-ON of an individual DAB is retained as the resonant current does not affect the commutation currents between the top and bottom devices.

Fig. 9 shows the transient waveforms of the AB-ISOP during power reversal from +600 to −200 W, including the output voltage and current (V_{out} and I_{out}), the ac-link current of different modules ($i_{ac,1}$, $i_{ac,2}$, and $i_{ac,3}$), the input module voltages ($V_{in,1}$, $V_{in,2}$, and $V_{in,3}$), and the resonant currents through the NRDABs

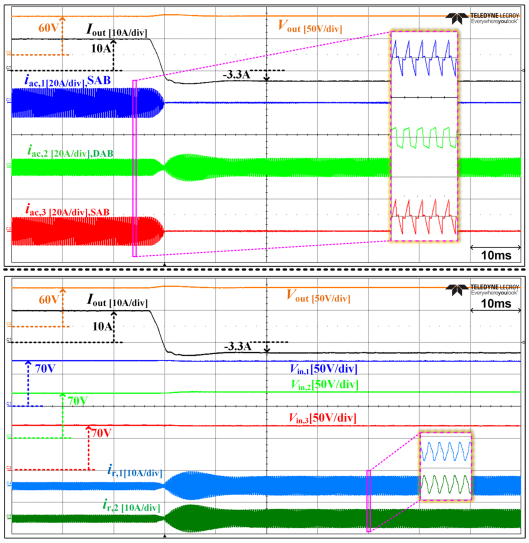

Fig. 9. Transient waveforms of the AB-ISOP during power reversal.

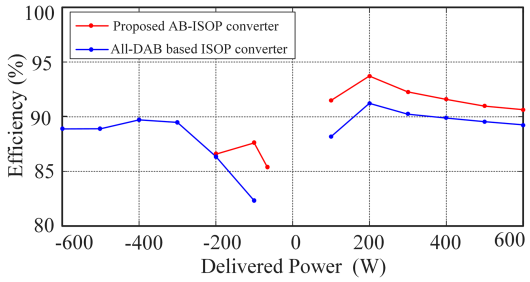

Fig. 10. Efficiency comparison with the all-DAB-based ISOP converter.

($i_{r,1}$ and $i_{r,2}$). As observed, the output voltage V_{out} is stabilized at 60 V by the AB-ISOP when the output current I_{out} drops from 10 to 0 A and increases in the opposite direction. After entering the backward mode, the SAB modules stand by with their transformer currents clamped at 0, and the DAB module is responsible for the reversed power transfer. Meanwhile, the resonant currents of NRDABs ($i_{r,1}$ and $i_{r,2}$) are automatically initiated to process power mismatches among the DAB and SAB modules. In both steady-state and transition modes, the module voltages at the input side are well-balanced without apparent deviation. These results confirm the seamless power reversal property and natural module voltage-sharing capability of the proposed AB-ISOP converter.

Fig. 10 compares the measured efficiency of prototypes based on the AB-ISOP topology and the conventional ISOP converter constituted purely by the DAB modules. The two prototypes are constructed with the same power stacks and transformers and operated under the same conditions. The proposed converter presents apparent efficiency improvement thanks to eliminating power losses associated with active devices at the secondary side of SAB modules, fewer devices and transformers conducting current under reversed mode, and soft-switching features of the embedded NRDABs. Although the measured efficiency is not high, as the proof-of-concept prototype has not been optimized for efficiency, the comparison results show the superiority of the proposed topology.

VI. Conclusion

Aimed to satisfy the realistic requirement for interlinking the MV and LV buses in the dc distribution grid, this letter has presented an AB-ISOP converter composed of SAB and DAB modules, with the NRDAB chain embedded at the input stage for natural power coupling and voltage sharing. Compared with the all-DAB-based ISOP, the proposed one requires fewer devices and shows higher conversion efficiency.

References

[1] R. W. De Doncker, "Power electronic technologies for flexible dc distribution grids," in *Proc. IEEE Int. Power Electron. Conf.*, 2014, pp. 736–743.

[2] M. Stieneker and R. W. De Doncker, "Medium-voltage dc distribution grids in urban areas," in *Proc. IEEE 7th Int. Symp. Power Electron. Distrib. Gener. Syst.*, 2016, pp. 1–7.

[3] E. Rodriguez-Diaz, J. C. Vasquez, and J. M. Guerrero, "Intelligent dc homes in future sustainable energy systems: When efficiency and intelligence work together," *IEEE Consum. Electron. Mag.*, vol. 5, no. 1, pp. 74–80, Jan. 2016.

[4] J. Hu, Y. Zhang, S. Cui, P. Joebges, and R. W. De Doncker, "A partial-power regulated hybrid modular dc-dc converter to interconnect MVDC and LVDC grids," in *Proc. IEEE 10th Int. Symp. Power Electron. Distrib. Gener. Syst.*, 2019, pp. 1030–1035.

[5] G. De Carne, G. Buticchi, Z. Zou, and M. Liserre, "Reverse power flow control in a ST-fed distribution grid," *IEEE Trans. Smart Grid*, vol. 9, no. 4, pp. 3811–3819, Jul. 2018.

[6] C. Meyer, "Key components for future offshore dc grids," Ph.D. dissertation, Inst. Power Electron. Elect. Drives, RWTH Aachen Univ., Aachen, Germany, 2007.

[7] R. Zhu, F. Hoffmann, N. Vázquez, K. Wang, and M. Liserre, "Asymmetrical bidirectional dc–dc converter with limited reverse power rating in smart transformer," *IEEE Trans. Power Electron.*, vol. 35, no. 7, pp. 6895–6905, Jul. 2020.

[8] J. Yao, W. Chen, C. Xue, Y. Yuan, and T. Wang, "An ISOP hybrid dc transformer combining multiple SRCs and DAB converters to interconnect MVDC and LVDC distribution networks," *IEEE Trans. Power Electron.*, vol. 35, no. 11, pp. 11442–11452, Nov. 2020.

[9] C. Mi, H. Bai, C. Wang, and S. Gargies, "Operation, design and control of dual H-bridge-based isolated bidirectional DC–DC converter," *IET Power Electron.*, vol. 1, no. 4, pp. 507–517, Apr. 2008.

[10] Y. Ting, S. de Haan, and B. Ferreira, "Modular single-active bridge DC-DC converters: Efficiency optimization over a wide load range," *IEEE Ind. Appl. Mag.*, vol. 22, no. 5, pp. 43–52, Sep./Oct. 2016.

[11] L. Li, G. Xu, D. Sha, Y. Liu, Y. Sun, and M. Su, "Review of dual active bridge converters with topological modifications," *IEEE Trans. Power Electron.*, vol. 38, no. 7, pp. 9046–9076, Jul. 2023.

[12] C. Sun, M. Zhu, X. Zhang, J. Huang, and X. Cai, "Output-series modular dc–dc converter with self-voltage balancing for integrating variable energy sources," *IEEE Trans. Power Electron.*, vol. 35, no. 11, pp. 11321–11327, Nov. 2020.

[13] C. Sun, X. Zhang, J. Zhang, M. Zhu, and J. Huang, "Hybrid input-series–output-series modular dc–dc converter constituted by resonant and nonresonant dual active bridge modules," *IEEE Trans. Ind. Electron.*, vol. 69, no. 1, pp. 1062–1069, Jan. 2021.

[14] Y. Yuanmao and K. W. E. Cheng, "Zero-current switching switched-capacitor zero-voltage-gap automatic equalization system for series battery string," *IEEE Trans. Power Electron.*, vol. 27, no. 7, pp. 3234–3242, Jul. 2012.

[15] J. T. Stauth, M. D. Seeman, and K. Kesarwani, "Resonant switched-capacitor converters for sub-module distributed photovoltaic power management," *IEEE Trans. Power Electron.*, vol. 28, no. 3, pp. 1189–1198, Mar. 2013.

[16] J. Zhang, J. Liu, J. Yang, N. Zhao, Y. Wang, and T. Q. Zheng, "A modified dc power electronic transformer based on series connection of full-bridge converters," *IEEE Trans. Power Electron.*, vol. 34, no. 3, pp. 2119–2133, Mar. 2019.

[17] J. Huang, J. Xiao, C. Wen, P. Wang, and A. Zhang, "Implementation of bidirectional resonant DC transformer in hybrid AC/DC microgrid," *IEEE Trans. Smart Grid*, vol. 10, no. 2, pp. 1532–1542, Mar. 2019.